

Food Science and Applied Biotechnology

e-ISSN: 2603-3380

Journal home page: www.ijfsab.com
<https://doi.org/10.30721/fsab2018.v1.i1>



Research Article

Structural Anomalies in Stirred Submerged Bioreactors Relevant to Immersed Membrane Use

Serafim D. Vlaev¹✉, Iren Tsibranska¹, Daniela Dzhonova-Atanasova¹, Roman Popov¹

¹Institute of Chemical Engineering at the Bulgarian Academy of Sciences, Acad. G. Bonchev Str. Bl. 103, 1113 Sofia, Bulgaria

Abstract

Separation of value-added food additives is often practiced by micro and ultrafiltration membranes in integrated submerged membrane bioreactors (sMBR) and the flow conditions are of major importance for their performance. The immersed membranes affect fluid circulation and may cause operational difficulties. Such malfunction termed flow structural deterioration of integrated vessels is addressed in this study, based on the effect of the (1) non-Newtonian component presence, and the (2) gas flow rate. Ranges of input parameters referring to power law non-Newtonian fluids with consistency coefficients of 0.02 to 0.1 Pa.sⁿ (flow index $n < 1$) and gas flow rate 1 - 2 vvm are studied. Computational fluid dynamics (CFD) simulation of a dual impeller bioreactor equipped with a mono-tubular membrane module and alternatively flat-blade or curved-blade impellers was carried out. 3-D “k-ε” turbulent flow model is used and 2-D contour plots are worked out to illustrate cases of restricted fluid mobility in the vicinity of membrane walls. The corresponding performance parameters, gas volume fraction and fluid surface velocity are discussed. Flow structural anomalies referring to zones at the immersed membranes of extremely low membrane surface velocity ($< 1 \text{ mm} \cdot \text{s}^{-1}$) and velocity gradients ($< 10 \text{ s}^{-1}$) that are risky for membrane fouling are uncovered.

Practical applications. Fermentation of food ingredients in stirred vessels combined with recovery of the value-added product is the target application. Examples are the production and recovery of peptides, gums' (gelatin, pectin) concentration, production of fructooligosaccharides, galactoglucomannan, enzymatic hydrolysis combined with selective ultrafiltration in processing of vegetable proteins, production of antioxidants. Viscous dispersions of food ingredients such as starch or xanthan and operating variables - impeller speed, rate of gassing - at various level may cause undesirable effects in the bioreactor flow uniformity leading to decrease of membrane separation efficiency. The cases engaging process fluids of high consistency such as exopolysaccharide dispersions are specific in this category. Restricted fluid mobility in the vicinity of the membrane module reduces the rate of fusion across the membrane surface and blocks up the product recovery. The resulting membrane fouling and the flow structural anomalies adhere to the problem of fouling control and to submerged membrane bioreactor applications.

Keywords: mixing, MBR, restricted fluid flow, CFD model analysis, membrane fouling

Abbreviations: sMBR – submerged membrane bioreactors; CFD – computational fluid dynamics; FBI – flat-blade radial flow impeller; MVI – arc-blade backswept impeller; RANS - Reynolds-averaged Navier-Stokes; MV – multi-vortex

✉ Corresponding author: Prof. Serafim Vlaev, DSc; Chemical and Biochemical Reactor Lab, Institute of Chemical Engineering, Acad. G. Bonchev Str. Bl. 103, 1113 Sofia, Bulgaria, tel. +359 28 70 32 73; E-mail: mixreac@gmail.com

Article history:

Received 5 December 2017

Reviewed 7 January 2018

Accepted 19 January 2018

Available on-line 14 March 2018

<https://doi.org/10.30721/fsab2018.v1.i1.12>

© 2018 The Authors. UFT Academic publishing house, Plovdiv

Introduction

Separation of value-added food additives is often practiced by micro and ultrafiltration membranes in integrated submerged membrane bioreactors (sMBR) and the flow conditions are of major importance for their performance. The membrane bioreactor (MBR) is the advanced process unit that integrates a biological reaction process and a separation membrane process avoiding inhibitory effects in the fermentation and allowing selective removal of a desired product. Major advantages of such system are its good sustainability, lower energy and material use and good productivity (Dalmau et al. 2014; Larroche et al. 2017). Examples are the production and recovery of functional polysaccharides (Mazzei et al. 2010; Camelini et al. 2013), lipase, rhamnolipid (Dhariwal thesis) peptides, gelatine and pectin (Lipnizki 2010), production of fatty acids (Chakraborty et al. 2012) fructooligosaccharides (Sanchez et al. 2008), galactoglucomannan (Persson and Johnsson 2010), the enzymatic hydrolysis combined with selective ultrafiltration in processing of vegetable proteins (Dauffin et al. 2001) and also other (Giorno et al. 2017). Despite its obvious advantages, the process has a major drawback due to the problem of membrane fouling. The need for fouling control is a condition for proper production. Various methods for fouling reduction have been accomplished including means for turbulence intensification; stirred vessels with turbulent impellers and aeration have been proposed (Fane 2008; Böhm et al. 2012). Referring to fermentation and food processing, they are eminent also because of the complex media involved. Due to high consistency of the food processing fluid, fouling often persist to be a hard operational problem. Complex hydrodynamics in sMBR may lead to restricted fluid mobility and cause difficulties in both the fermentation reaction and the product recovery. The level of input variables in food processing vessels involved in integrated processing could generate critical conditions that should be revealed in advance in order to avoid problems of inefficient product recovery. As part of a more extended analysis, the study objective is to exemplify extreme cases of sMBR hydrodynamic performance suspect of membrane malfunction and to specify input

parameters subject to the performance anomalies observed.

Materials and Methods

Material model systems. For the purpose of the study, two systems containing polysaccharides of extreme viscosity, a water-like similar in consistency and content to a system producing exopolysaccharide by extremophilic yeast (Vlaev et al. 2013) and a highly viscous non-Newtonian one (Demirci et al. 2017) were assumed to be the physical models. Rheometer Rheotest 2 (MLW, Medingen, Germany) was used to register the flow curves of the original bioreaction models. The fluids were found to obey the power law model of pseudoplastic solutions with flow properties estimated by consistency coefficient, K , and flow index, n , as follows: $0.02 \text{ Pa}\cdot\text{s}^n$ and 0.78 for the water-like liquid and $0.1 \text{ Pa}\cdot\text{s}^n$ and 0.78 for the highly viscous one.

Production/separation unit set-up. The simulated bioreactor is a dual impeller 5L fermentation stirred vessel of the type used in a previous study (Pavlova et al. 2011). A schematic of the vessel set-up is shown in Fig.1a. The vessel performance corresponding to two different impeller designs (Fig. 1b), namely, a flat-blade radial flow impeller (indicated as FBI) and an arc-blade backswept impeller (MVI) (Vlaev and Georgiev 2014) was

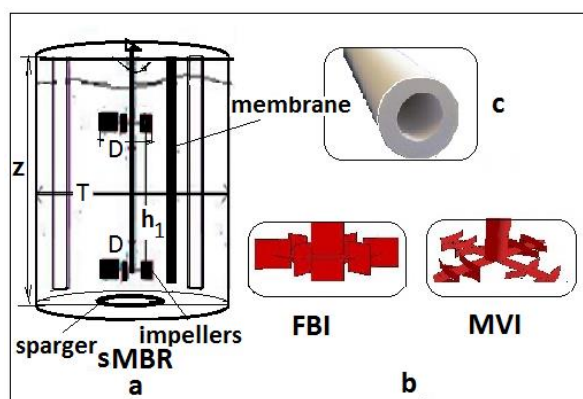


Figure 1. Experimental set-up: sMBR (a), impellers (b) and membrane (c)

considered. The integrated vessel design included a tubular membrane module mounted on the top of the vessel and positioned vertically from top to bottom at a distance of 14cm from the vessel wall.

The membrane tube was 12mm in diameter and 23cm long. The membrane module was a tubular mono-channel, similar to the type produced by ItN Nanovation (pore size 0.6-0.8 μ m) used for microfiltration in fermentation (Dhariwal 2007) (Fig. 1c).

Mathematical modeling and simulation. Because of the complexity of the system, computational simulation and visualization using Navier-Stokes models and CFD technique were employed. The simulations were based on the specific stirred vessel geometry and on the model of two-phase gas-liquid turbulent flow (Vlaev et al. 2012).

Hydrodynamic model. The Euler-Euler model was used to describe the gas-liquid flow. A 3-D Reynolds-Averaged Navier-Stokes (RANS) model was employed. The governing mass and momentum conservation equations were assumed per phase. Turbulence was modelled by the realizable "k- ϵ " model with the corresponding transport equations for k and ϵ . The MRF approach was used for the rotating parts. A rotating frame of the same rotational speed as the impeller was used for the inner region and a stationary frame for the domain. The grid contained ca. 0.9x10⁶ cells. Grid dependency was tested by two different steps of refinement.

Simulation details. CFD simulation analysis of the structural changes in the mixing bioreactor was accomplished. Fluent (ANSYS FLUENT Release 13.0, ANSYS, Inc. 2010) was used to solve the governing equations of the gas-liquid two phase flow field numerically. The boundary conditions were pressure outlet for the bed top with 100 percent gas volume fraction for the gas phase, and velocity inlet with 100 per cent gas volume fraction and gas linear velocity at z-component of 8-16m.s⁻¹ corresponding to the selected gas flow rate and sparger dimensions. Unsteady solution was performed with initial time step of 0.001s. The convergence criterion was set for the velocities and turbulence values equally at 1x10⁻⁵. A reasonable convergence was achieved. Validation was carried out by basic parameters, mainly gas volume fraction and strain rate, as well as by comparing values of experimental and predicted wall shear rates. The simulation in this format has been experienced formerly and its validation related to

non-Newtonian flow has been reported in a previous study (Vlaev et al. 2012).

Results and Discussion

Case of pseudoplastic component presence. The hydrodynamic response of the model system, i.e. reactor and fluid, to extreme changes in consistency and apparent viscosity was examined. The surface velocity at the membrane module surface was registered. Velocity contours and angular-longitudinal distribution of velocity point values across the membrane tube obtained by CFD are shown in Fig. 2a and Fig. 2b, respectively.

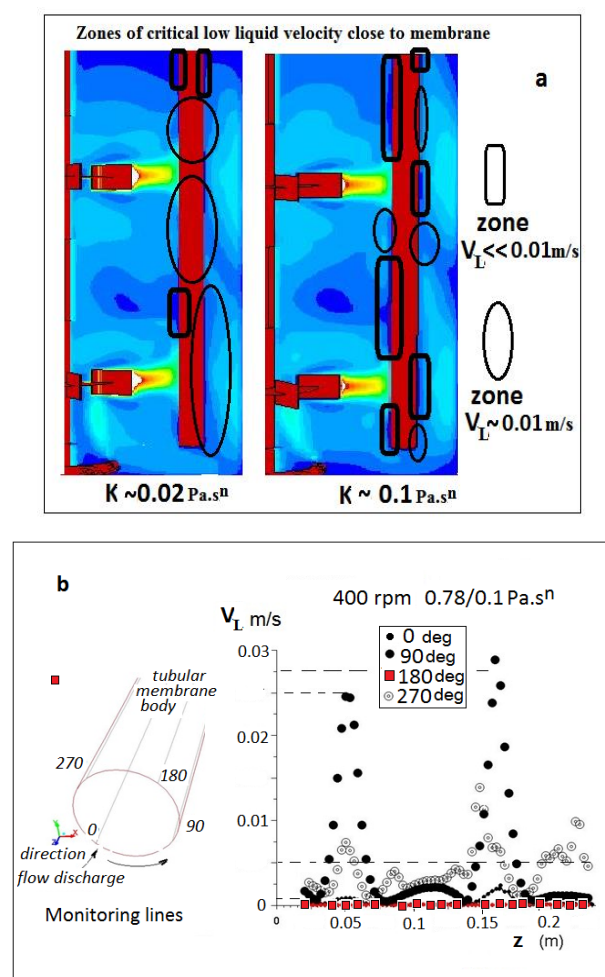


Figure 2. Uncovering the effect of consistency on membrane surface velocity: (a) Changes in liquid velocity in the bulk fluid at the membrane interface along the monitoring lines; (b) Angular variation of membrane near-wall surface liquid velocity V_L at extreme consistency.

The plot illustrates the membrane surface velocity at the two extremes of apparent viscosity. The zones of very low velocity ($V_L < 1 \text{ mm} \cdot \text{s}^{-1}$) in the vicinity of the membrane are outlined and shown to be extended in the case of high consistency coefficient $K = 0.1 \text{ Pa} \cdot \text{s}^n$. A zone of zero surface liquid velocity, corresponding to membrane rear (180deg), is marked with the square symbols.

Case of excessive gassing. The gas flow rate was changed from $4.5 \text{ dm}^3 \cdot \text{min}^{-1}$ to $9 \text{ dm}^3 \cdot \text{min}^{-1}$, corresponding to bulk volume-relative gas flow rate of 1vvm and 2vvm, respectively. The 2D-velocity contours and the angular distribution of surface velocity are plotted in Fig. 3.

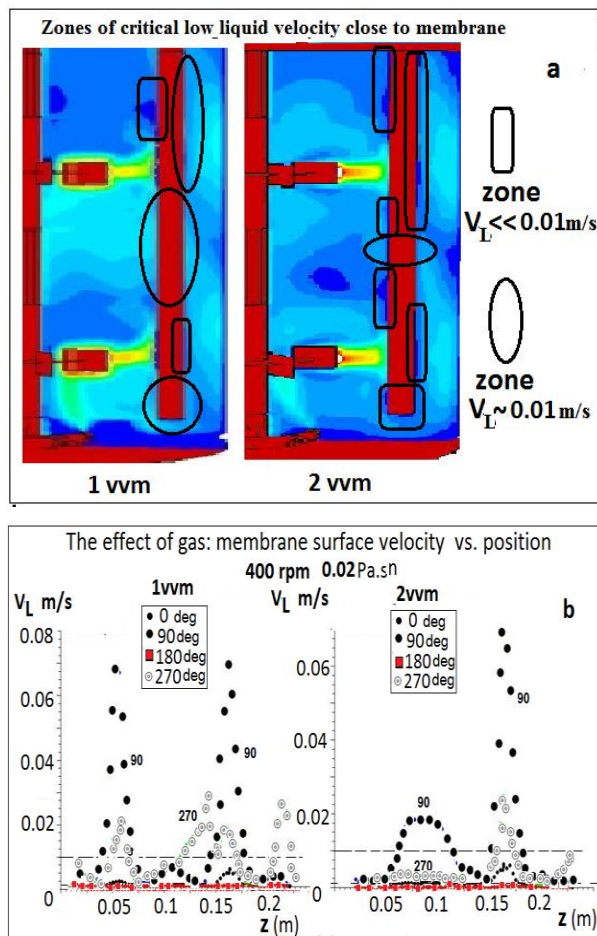


Figure 3. Uncovering the effect of gassing on the membrane surface velocity: (a) Changes in liquid velocity in the bulk fluid at the membrane interface, (b) Angular variation of membrane surface velocity in the process fluids at extreme gas sparging.

Structural anomalies are observed as located especially at the lower impeller at $z = 0.05 \text{ m}$. The overall membrane surface liquid velocity at gassing falls 3-fold from $7 \text{ cm} \cdot \text{s}^{-1}$ to $2 \text{ cm} \cdot \text{s}^{-1}$. In both cases an essential decrease of membrane shear rate is observed, as illustrated in Fig. 4.

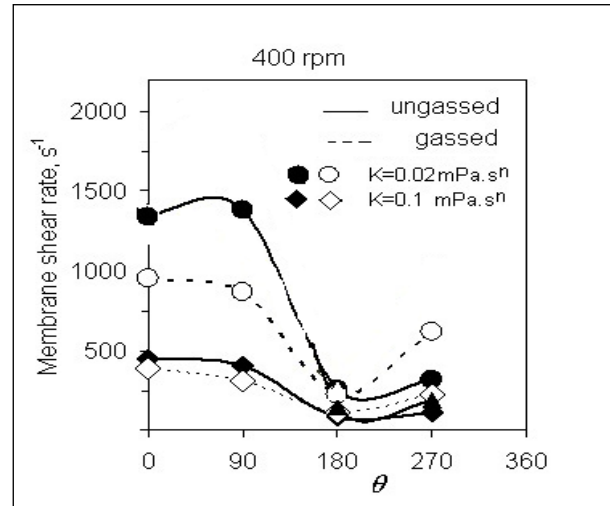


Figure 4. The effect of extreme conditions (consistency and gas flow rate) on membrane surface average-shear rate at various angle of the symmetry plane: frontal (0deg), side (90deg), rear (180deg) and side (270deg).

The figure shows the angular distribution of the average shear rate at the two extremes of apparent viscosity and gas flow velocity. The four average shear rate values are calculated as line-averaged values of the four monitoring lines, drawn along the generatrix of the membrane cylinder at a step of 90 degrees starting from the point facing the impellers, as shown in Fig. 2b (left). Based on a total set of additional data (not shown!) the ranges of input parameters referring to power law non-Newtonian fluids that could lead to membrane malfunction were determined, as of any flow index $n < 1$ at consistency $\sim 0.1 \text{ Pa} \cdot \text{s}^n$ as well as gas flow rates exceeding 1vvm. The corresponding performance parameters - gas volume fraction, apparent viscosity distribution and variation of the gas cloud - that could explain the performance of restricted fluid mobility in the vicinity of membrane walls were considered. The obvious result of shear depression cannot be explained by gas effect on velocity, since in fact gas velocity imparts additional moment to the liquid flow at the

membrane interface. It should not be due also to the impeller rpm, since the membrane is positioned in the area of high turbulence.

The explanation of the malfunction estimated as low membrane surface velocity should be due to the highly pseudoplastic behavior of the dispersion at $n \sim 0.78$, $K \sim 0.1 \text{ Pa}\cdot\text{s}^n$ that reduces the fluid motion at the interface and causes changes in the two-phase flow structure. Visualization of the apparent viscosity distribution in 2-D is shown in Fig. 5

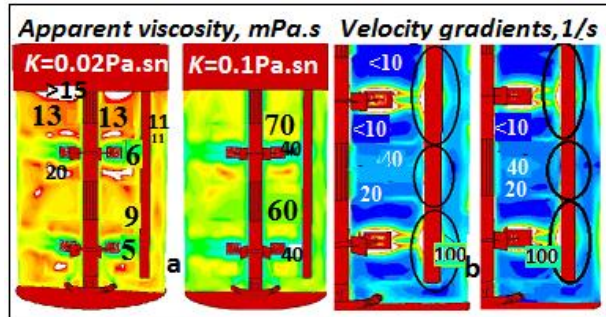


Figure 5. Structural changes in the sMBR flow field encompassing the membrane module at 5-fold viscosity increase: (a) 2-D apparent viscosity contours (in mPa.s) at consistency rise from $0.02 \text{ Pa}\cdot\text{s}^n$ to $0.1 \text{ Pa}\cdot\text{s}^n$; (b) The corresponding velocity gradient contours (in s^{-1}).

In support of the above deduction, further numerical analysis was carried out and the following evidence data was found (Fig. 6).

(1) The liquid volume fraction at the membrane surface was registered to be extremely low at high consistency; A gas cloud at the membrane surface, e.g. gas holdup of 17-19% seems to be formed (Fig. 6a). (2) On the other hand, gas bypass is seen clearly to be formed at 2vvm (Fig. 6b) and a big portion of the liquid at the membrane surface remains unaffected by the gas presence. Both component relationships point at a change in the gas-liquid flow structure in a way that the membrane is in contact with a low-motion fluid that increases the risk of fouling. To summarize, two types of anomalies due to (1) pronounced non-Newtonian fluid behavior (A), and (2) high gas flow rate (B), were registered. Input parameters (consistency coefficient, impeller speed and tip velocity, gas flow rate) and resulting average and maximum shear rates are summarized in Table 1 and can be discussed in the sense of reactor theory

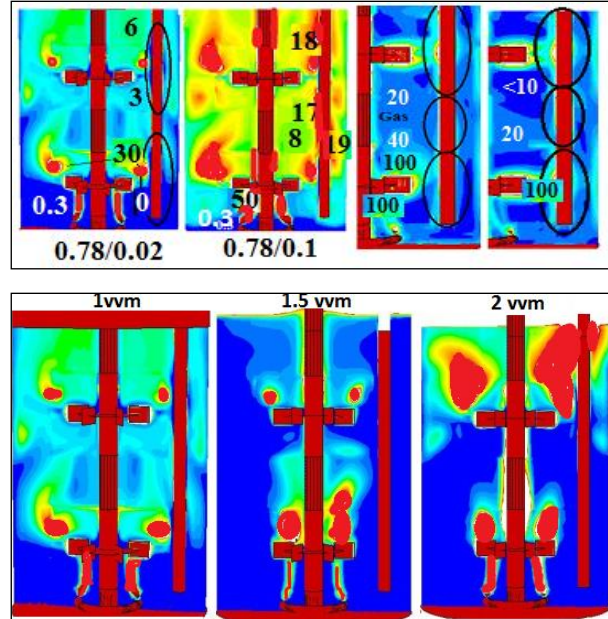


Figure 6. (a) Variation of gas volume fraction (in %) distribution with consistency at 1vvm and corresponding changes in zonal shear rate (in s^{-1}); (b) Visualized variation of gas volume fraction distribution with sparging rate at consistency coefficient $0.02 \text{ Pa}\cdot\text{s}^n$.

1vvm-max effect of gas velocity on shear,

1.5 vvm -negligible effect of gas velocity on shear,

2vvm - bypass of the gas effects only the upper membrane section

(Buwa et al. 2016). Cases A and B were termed structural anomalies or flow “pathology”, as they hinder fluid motion and decrease mass transport across the membrane. By generalization, the low fluid mobility conditions become risky for fouling. Since the physical parameters of such operation are realistic, means of remedy to such anomalies has to be found, in order to achieve effective performance. Based on reference data for the impeller MVI (Vlaev and Dzhonova 2017), a remedy to the conditions related to flat blades has been proposed by introducing a different impeller design by impeller blade retrofitting: replacement of the flat blades with curved blades. The curved blades are reported to produce a multi-vortex (MV) of the backswept type of flow pattern accompanied by different flow velocity distribution along the membrane-fluid interface, as reported earlier (Vlaev and Georgiev 2014). Our observations show that an improved velocity gradient could be

obtained. Table 1 contains the results, including the data of MVI performance. Obviously, by changing the impeller type the detrimental effect of fluid high viscosity and excessive gassing could be balanced for an enhanced shear profile to be obtained.

Table 1. Summary of parameters marking anomalies for flat blades (FBI) and suggested improvement by retrofitting (MVI)

| Fluid property, K, Pa.s ⁿ /n | Impeller speed/ Tip velocity, rpm/m.s ⁻¹ | Gas flow rate, vvm | Average shear rate, ks ⁻¹ | Max shear rate, ks ⁻¹ |
|---|---|--------------------|--------------------------------------|----------------------------------|
| <i>In case of FBI</i> | | | | |
| 0.02/0.78 | 400/1.4 | 0 | 0.936 | 12.9 |
| 0.02/0.78 | - | 1 | 0.871 | 12.85 |
| 0.02/0.78 | - | 1.5 | 0.606 | 5.78 |
| 0.02/0.78 | - | 2 | 0.631 | 9.18 |
| 0.1/0.78 | - | 0 | 0.283 | 3.96 |
| 0.1/0.78 | - | 1 | 0.352 | 6.67 |
| <i>In case of MVI</i> | | | | |
| 0.02/0.78 | 750/2.6 | 0 | 0.96 | 7.3 |
| 0.02/0.78 | - | 1 | 0.93 | 7.3 |
| 0.1/0.78 | - | 0 | 0.437 | 3.4 |
| 0.1/0.78 | - | 1 | 0.576 | 3.7 |

Conclusions

Stirred sMBR require flow pattern uniformity and circulation/cross-flow velocity intensive enough to generate high velocity gradients at the membrane interface for the sake of good fouling control and proper membrane operation. Food ingredients in the process fluid often impart non-Newtonian behavior to the fluid, the flow structure being additionally influenced by the impeller speed and gas sparging intensity. Referring to such conditions in the bioreactor, this study proves the occurrence of zones of very low membrane surface velocities (<1mm.s⁻¹ compared to 1400mm.s⁻¹ at the impeller tip) and velocity gradients (<10s⁻¹), increasing the risk of fouling. Based on previous knowledge on the characteristics of curved blades, fouling remedy by retrofitting impeller design is proposed.

Acknowledgements

This work is supported by the National Science Fund at the Ministry of Education and Science under Contract DN 07/11-15.12.2016. The authors' budget quota is confirmed.

References

- Bohm, L., Drews A., Prieske H., Berube P. R., Kraume M. The importance of fluid dynamics for MBR fouling mitigation. *Bioresource Technology*, 2012, 122(10): 50-61.
<https://doi.org/10.1016/j.biortech.2012.05.069>
- Buwa, V. V., Roy Sh., Ranade V. V. Three-phase slurry reactors. Chapter 6. In: *Multiphase Catalytic Reactors: Theory, Design, Manufacturing and Applications* (Z. I. Onsan, A. K. Avci, Eds.). Wiley, New Jersey. 2016, pp. 132-156, Print ISBN: 9781118115763, Online ISBN: 9781119248491,
<https://doi.org/10.1002/9781119248491>
- Camelini, M., Rezzadori K., Benedetti S., Proner M. C., Fogaça L., Azambuja A. A., Giachini A. J., Rossi M. J., Petrus J. C. C. Nanofiltration of polysaccharides from *Agaricus subrufescens*. *Applied Microbiology and Biotechnology*, 2013, 97(23): 9993-10002.
<http://doi.org/10.1007/s00253-013-5241-y>
- Chakraborty, S., Drioli E., Giorno L. Development of a two separate phase submerged biocatalytic membrane reactor for the production of fatty acids and glycerol from residual vegetable oil streams. *Biomass and Bioenergy*, 2012, 46(11): 574-558.
<https://doi.org/10.1016/j.biombioe.2012.07.004>
- Dalmau, M., Monclús H., Gabarrón S., Rodriguez-Roda I., Comas J. Towards integrated operation of membrane bioreactors: Effects of aeration on biological and filtration performance. *Bioresource Technology*, 2014, 171(11): 103-112.
<http://doi.org/10.1016/j.biortech.2014.08.031>
- Daufin, D., Escudier J.-P., Carre H., Re Á., Bearot S., Fillaudeau L., Decloux M. Recent and emerging applications of membrane processes in the food and dairy industry. *Food and Bioproducts Processing*, 2001, 79(2): 89-102.
<https://doi.org/10.1205/096030801750286131>
- Demirci, A. S., Palabiyık I., Deniz A. D., Apaydin D., Gümüs T. Yield and rheological properties of exopolysaccharide from a local isolate: *Xanthomonas axonopodis*. *Electronic Journal of Biotechnology*, 2017, 29(11): 18-23.
<https://doi.org/10.1016/j.ejbt.2017.08.004>
- Dhariwal, A. The significance of submerged ceramic membrane systems for production oriented bioprocesses. PhD Thesis, Fakultät 8-Naturwissenschaftlich-Technische Fakultät III, University of Saarland, 2007 [in German]
- Fane, A.G. Submerged membranes. Chapter 10. In: *Advanced Membrane Technology and Applications* (N.N. Li, A.G. Fane, W.S. Winston-Ho, T. Matsuura, Eds.). Wiley, New Jersey. 2008, pp. 239-270, Print ISBN: 9780471731672, Online ISBN: 9780470276280,
<https://doi.org/10.1002/9780470276280>
- Giorno L., Mazzei R., Piacentini E., Drioli E. Food application of membranes. Chapter 9 In: *Engineering Aspects of Membrane Separation and Application in Food Processing* (R. Field, E. Bekassy-Molnar, F. Lipnizki, G. Vatai Eds.). Taylor & Francis Group CRC Press, Boca Raton, Florida. 2017, pp. 299-360, Print ISBN-10: 1420083635, Online ISBN-13: 978-1420083637

- Coutte F., Leciuturier D., Firdaous L., Kapel R., Bazinet L., Cabassud C., Dhulster P. Recent Trends in Membrane Bioreactors. Chapter 10 In: *Current Developments in Biotechnology and Bioengineering. Bioprocesses, Bioreactors and Controls*. (Ch. Larroche, M. A. Sanroman, G. Du, A. Pandey Eds.). Elsevier Ltd., Amsterdam. 2017, pp. 279-303, ISBN: 978-0-444-63663-8.
- Lipnizki, F. Cross-flow membrane applications in the food industry. Chapter 1 In: *Membrane technology. Volume 3: Membranes for food applications* (K-V. Peinemann, S. P. Nunes, L. Giorno Eds.). Wiley-VCH Verlag, Weinheim. 2010 pp. 1-2. ISBN: 978-3-527-31482-9.
- Pavlova K., Rusinova-Videva S., Kuncheva M., Kratchanova M., Gocheva M., Dimitrova S. Synthesis and characterization of an exopolysaccharide by Antarctic yeast strain *Cryptococcus laurentii* AL100. *Applied Biochemistry and Biotechnology*, 2011, 163(8): 1038-1052.
<https://doi.org/10.1007/s12010-010-9107-9>
- Persson, T., Jönsson A. S. Isolation of hemi-celluloses by ultrafiltration of thermomechanical pulp mill process water. Influence of operating conditions. *Chemical Engineering Research and Design*, 2010, 88(12): 1548-1554.
<https://doi.org/10.1016/j.cherd.2010.04.002>
- Sanchez, O., Guio F., Garcia D., Silva E., Caicedo L. Fructooligosaccharides production by *Aspergillus* sp. N74 in a mechanically agitated airlift reactor. *Food and Bioprocess Processing*, 2008, 86(2): 109-115.
<https://doi.org/10.1016/j.fbp.2008.02.003>
- Vlaev, S. D., Dzhonova-Atanasova D. Local velocity and shear deformation rate at model membranes immersed in a bioreactor agitated by curved blade impeller: The effect of membrane position. *Materials, Methods & Technologies - Journal of International Scientific Publications*, 2017, 11(1): 216-229.
<https://www.scientific-publications.net/get/1000024/1501345687848973.pdf>
- Vlaev, S. D., Georgiev D. CFD-characterization of the MV-impeller related to polysaccharide dispersion mixing, *Scientific Works of University of Food Technologies*, 2014, 61(1): 745-749.
http://eprints.ugd.edu.mk/12478/1/ScienWork_2014-2.pdf
- Vlaev, S. D., Martinov M., Georgiev D. RANS-modeling of macroparameter distribution in dual impeller stirred bioreactors for ESP production. *Scientific Works of University of Food Technologies*, 2012, 53(1): 840-845 [in Bulgarian]
- Vlaev S. D., Rusinova-Videva S., Pavlova K., Kuncheva M., Panchev I., Dobрева S. Submerge culture process for biomass and exopolysaccharide production by Antarctic yeast: some engineering considerations. *Applied Microbiology and Biotechnology*, 2013, 97(12): 5303–5313.